Improving battery pack model accuracy of next-generation light-duty battery electric trucks under JE05 driving cycle

- Lookup Table Generated from an Electrochemical Cell Model with Temperature Consideration -

Xinwei Li [1)] Haoxiang Li [1)] Ratnak Sok [1, *)] Keiki Tanabe[2)] Goro Iijima[2)] Jin Kusaka [1)]

1) Propulsion and Energy Systems Laboratory, Waseda University, Shinjuku, Tokyo, Japan

*E-mail: * ratnak@ruri.waseda.jp*

2) Mitsubishi FUSO Truck & Bus Corporation, Tochigi, Japan

ABSTRACT: This paper proposes an electrochemical battery model for electric trucks, incorporating temperature effects to enhance simulation accuracy. The proposed model is compared with the conventional Internal Resistance (IR) look-up model to evaluate performance improvements. With its more detailed representation of battery dynamics, the electrochemical model, particularly under varying thermal conditions, demonstrates a higher prediction accuracy. Simulation results under JE05 driving conditions show that the proposed model improves the accuracy of voltage prediction, offering a more reliable tool for electric truck powertrain simulations.

KEY WORDS: Electric truck, Vehicle modeling, Open-source model, LFP Cathode, Electro-thermal model, State of charge

1. INTRODUCTION

Global warming is a critical issue worldwide, making it essential for countries to put every effort into reducing greenhouse gas emissions. Though vital for transporting goods, delivery trucks are major contributors to these emissions. Transitioning the traditional trucks to electric trucks offers a significant opportunity to lower emissions. According to the global electric truck market analysis(1), the market is projected to experience significant growth, with a compound annual growth rate (CAGR) of approximately 42.7% by 2035. To further encourage automobile energy conservation and emission reduction and combat global warming, the Ministry of Land, Infrastructure, Transport, and Tourism, (MLIT) has introduced new fuel efficiency standards for heavy-duty vehicles (including trucks and buses weighing more than 3.5 tons) with the target year of 2025, called the JH25 mode(2). Compared with the 2015 standards, the new standards will increase the fuel efficiency of trucks by 13.4% and buses by 14.3%. The JH25 electric vehicle test method applies to vehicles specified by guidelines. This test method uses a hardware-in-loop system (HILS) when driving in JE05 mode (referred to as 'Transient urban driving mode').

2. PROBLEM STATEMENT

Among all battery types, lithium-ion batteries are widely used for automotive applications due to their superior energy density and charging efficiency nowadays. A correct estimation of the battery's electrical and thermal dynamics plays an important role in operating safely and efficiently. Various model-based observer approaches have been widely explored to address this issue. In this paper, the verification aims to evaluate the accuracy of various battery models when driving according to the JE05 mode. In the internal resistance method, an important aspect missing is the effect of temperature on battery performance. Real-world battery charging and discharging processes involve complex electrochemical characteristics, which can significantly affect the voltage response. The model simplifies these processes and ignores important electrochemical effects such as electrode polarization or concentration polarization, which may result in lower simulated voltages than actual measurements. This comparison will be conducted between the general Internal Resistance (IR) look-up method and the electrochemical method, while calculating electrical models for state of charge (SOC) and voltage estimation(3) which combines a thermal model for temperature monitoring(4) (5) and offers a more detailed representation of battery characteristics. By coupling the electrochemical kinetics and the thermal behavior of the battery, the model significantly improves the accuracy under the JE05 driving cycle. Furthermore, since the model parameters correspond to physical phenomena, they can be more robustly determined from experimental data and adapted in real-time to

changes in battery state. Overall, this improved modeling approach enables more reliable simulation and control, ultimately leading to improved battery performance, higher safety margins and compliance with stringent heavy-duty vehicle operating standards.

3. SIMULATION MODEL

This section presents the schemes of the IR Model and the Dual-Polarization Equivalent Circuit Model. It provides further details on how to derive and optimize the parameters for battery representation.

3.1 Internal Resistance Model

The open-source internal resistance battery model downloaded from MLIT and the corresponding logic are shown in Figure 1 below. The main logic is to input the current to calculate the SOC of the battery and use it to determine the open-circuit voltage (OCV) and Internal Resistance (IR) [2].

The terminal voltage is calculated using Ohm's Law, and formulas are used to calculate the SOC, as shown below.

$$SOC = SOC_{initial} - \int_0^t \frac{I}{C_{nominal} \times 3600} dt \times 100 \quad (3.1)$$

$$U_t = U_{OCV} - \mathrm{I} \times R_0 \quad (3.2)$$

SOC: State of charge (%)

$SOC_{initial}$: Initial state of charge (%)

I: Battery current (A)

$C_{nominal}$: Battery capacity (Ah)

U_t: Battery terminal voltage (V)

U_{OCV}: Open circuit voltage (V)

R_0: Internal Resistance (Ω)

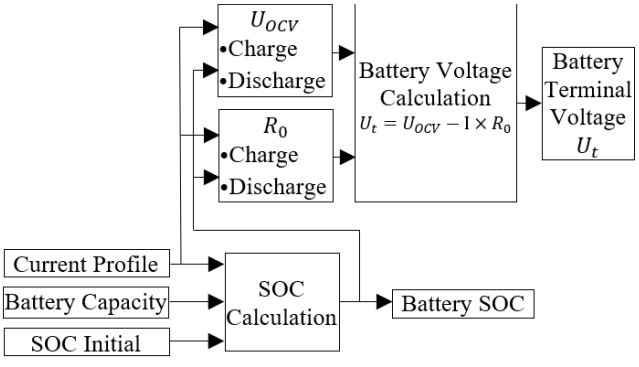

Fig. 1 Internal Resistance Battery Model and Logic

3.2 Battery Thermal Modelling

The schematic structure of the battery model with thermal effects is shown in Figure 2 below. The main principle of using the thermal model is to simulate the battery voltage by adding heat convection with coolant through the battery. Using the battery to generate heat and heat convection heat between the battery surface and coolant, the battery temperature can be calculated and input into the new model to determine the parameters.[6]

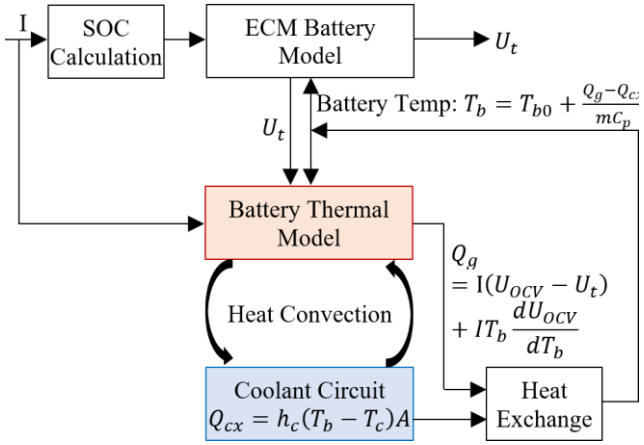

Fig. 2 Structure of the Battery Model with Thermal Effect

The heat generated by the battery is using the equation below:

$$Q_g = \mathrm{I}(U_{OCV} - U_t) + IT_{battery} \frac{dU_{OCV}}{dT_{battery}} \quad (3.3)$$

Q_g: Heat generation from battery (W)

$T_{battery}$: Battery temperature (K)

The heat convection between the battery and coolant is using the equation below:

$$Q_{convection} = h_{coolant}(T_{battery} - T_{coolant})A_{surface} \quad (3.4)$$

$Q_{convection}$: Heat generation from battery (W)

$h_{coolant}$: Coolant heat convection coefficient $(W/m^2.K)$

$A_{surface}$: Battery surface area (m^2)

where the coolant heat convection coefficient is calculated by Colburn Analogy[7] to calculate the wall heat transfer coefficient. The equation of Colburn Analogy is as follows:

$$h_{coolant} = \frac{1}{2} c_f . \rho . U_{eff} . c_p . (Pr)^{-\frac{2}{3}} \quad (3.5)$$

$h_{coolant}$: Calculated heat transfer coefficient $(W/m^2.K)$

c_f: Fanning friction factor of smooth pipe

ρ: Density of the coolant (kg/m^3)

U_{eff}: Effective velocity outside boundary layer (m/s)

C_p: Specific heat $(J/kg.K)$

Pr: Prandtl number

Therefore, the battery temperature variation is calculated based on the coolant's specific heat capacity and the battery's mass flow rate.

$$\Delta T_b = \frac{Q_g - Q_{cx}}{mC_p} \quad (3.6)$$

$$T_b = T_{b0} + \Delta T_{battery} \quad (3.7)$$

ΔT_b: Battery temperature change

For the battery model incorporating a thermal circuit, as illustrated in Figure 2, GT-SUITE was utilized to extract the battery's heat capacity. Additionally, the battery's heat generation and the coolant's convective heat transfer coefficient require optimization, as slight differences exist between the actual batteries used in the reference test batteries. The corresponding calibrated gain coefficients are denoted as k_1, k_2, k_3.

Battery heat capacity gain: $T_b = T_{b0} + \frac{Q_g{}' - Qcx}{k_1 \cdot c_{pb} \cdot m_b}$ (3.8)

Coolant heat convection gain:

$$Q_{cx} = k_2 \cdot h_c(T_b - T_c)A_{S,M,L} \quad (3.9)$$

Battery heat generation gain:

$$Q_g{}' = k_3 \cdot Q_g = k_3 \cdot (I(U_{OCV} - U_t) + IT_b \frac{dU_{ocv}}{dT_b}) \quad (3.10)$$

C_{pb}: Battery heat capacity $(J/kg.K)$

$A_{S,M,L}$: Battery surface area with S/M/L size battery specification (m^2)

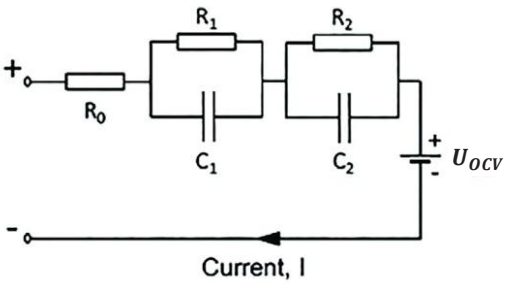

Fig. 3 2-RC Equivalent Circuit Model

The model is analyzed using the battery characterization module by using 2- RC circuits shown in Figure 3. [8] This is also called dual polarization model, based on the Thevenin model, further adds another 2 sets of RC networks to describe the polarization characteristics of the power battery.

$$\begin{cases} \dot{U_1} = -\frac{U_1}{R_1 C_1} + \frac{\mathrm{I}}{C_1} \\ \dot{U_2} = -\frac{U_2}{R_2 C_2} + \frac{\mathrm{I}}{C_2} \\ U_t = U_{ocv} - U_1 - U_2 - \mathrm{I} \times R_0 \end{cases} \quad (3.11)$$

After the characterization process, a 2D look-up table (LUT) is used to derive the equivalent circuit parameters under given conditions.

3.3 Model Parameterization

3.3.1 Model Parameterization for Internal Resistance Model

The battery test for internal resistance model[2] is conducted at 25degC according to the JH25 guideline, and the testing profile is shown in Figure 4. Figure 5 shows the calculation of IR and OCV. Characteristics obtained from the corresponding voltages are obtained by the least-squares method, in which the absolute value of the slope of the regression line is obtained as OCV, and the interception is obtained as IR.

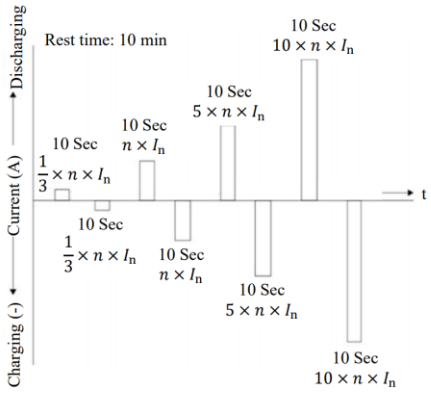

Fig. 4 Battery Testing Current Profile

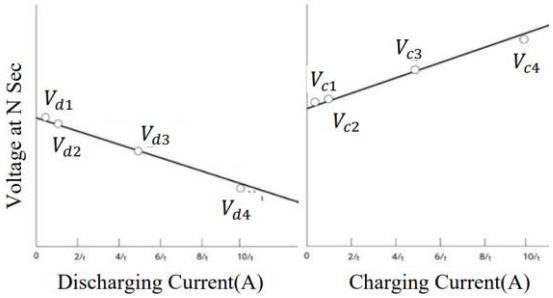

Fig. 5 Calculation of Internal Resistance and Open Circuit Voltage

3.3.2 Model Parameterization for Battery Thermal Modelling

A pseudo-two-dimensional (P2D) model based on the electrochemical approach was developed using GT-AutoLion 1D software with parameters. The electrochemical and thermodynamic properties of the battery considered from particle movement across the battery thickness and diffusion of particles across the radius direction. The P2D model phenomenon is shown in Figure 6, and the governing equations are shown below.[9]

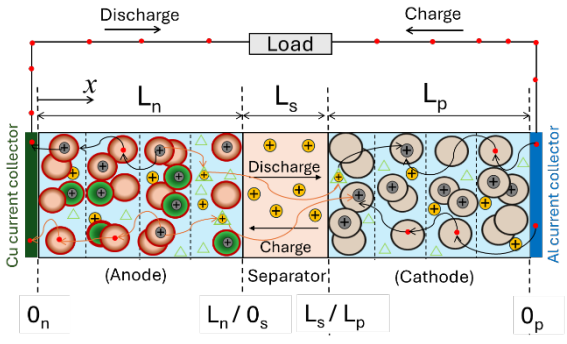

Fig. 6 Schematic of P2D Model [10-11]

According to Newman's P2D model[12], the current density and lithium-ion flux density are determined using the charge conservation equation (3.12).

Electric charge conservation:

$$\begin{cases} i_s + i_e = i = \dfrac{i_L}{S} \\ \dfrac{\partial \mathrm{i_e}}{\partial x} = a i_s = aFj_r \\ \dfrac{\partial \mathrm{i_s}}{\partial x} = -aFj_r \\ a_s = \dfrac{3\varepsilon_s}{R_s} \end{cases} \tag{3.12}$$

Lithium-ion concentration equations in liquid and solid phases:

Solid phase Lithium-ion diffusion calculation:

$$\frac{\partial C_s}{\partial x} = D_s\left(\frac{2}{r}\frac{\partial C_s}{\partial r} + \frac{\partial^2 C_s}{\partial r^2}\right) \tag{3.13}$$

Liquid phase Lithium-ion diffusion calculation:

$$\varepsilon_e \frac{\partial C_e}{\partial t} = \frac{\partial}{\partial x}\left(D_e^{eff}\frac{\partial C_e}{\partial x}\right) + a_s(1 - t_+^0)j_r \tag{3.14}$$

The electric potential Φ_e and Φ_s derived from Ohm's law equations (3.15) (3.16) with Li-ion concentrations C_e and C_s.

$$\sigma^{eff}\frac{\partial \Phi_s}{\partial x} - i_s = 0 \tag{3.15}$$

The interfacial overpotential ŋ between the solid and liquid phase is determined from the lithium-ion flux density j_r on the solid surface using Butler-Volmer equation (3.17).

Ohm's Law (Liquid phase):

$$k^{eff}\frac{\partial \varphi_e}{\partial x} + -\frac{2RTk_D^{eff}}{F}(t_+^0 - 1)\frac{\partial lnc_e}{\partial x} + i_e = 0 \tag{3.16}$$

Butler – Volmer equation:

$$\begin{cases} j_r = i_0\left(e^{\frac{\alpha_a F}{RT}\eta} - e^{\frac{\alpha_e F}{RT}\eta}\right) \\ i_0 = k_s C_e^{\alpha_a}\left(c_{s,max} - c_{surf}\right)^{\alpha_a} c_{surf}^{\alpha_e} \end{cases} \tag{3.17}$$

The potential difference in the solid phase between the positive and negative electrodes is used to determine the terminal voltage of the battery. As shown in equation (3.18), the solid phase potential is influenced by various factors, such as surface overpotential, liquid phase potential, steady-state open circuit voltage.

$$\begin{cases} V = \Phi_\mathrm{s}|_{x=x_p} - \Phi_\mathrm{s}|_{x=0} \\ \eta = \Phi_\mathrm{s} - \Phi_\mathrm{e} - V \end{cases} \tag{3.18}$$

Final terminal voltage equation:

$$V_t = \Phi_\mathrm{e}|_{x=x_p} - \Phi_\mathrm{e}|_{x=0} + \eta_p\big|_{x=x_p} - \eta_n|_{x=0} + V_p\big|_{x=x_p} - V_n|_{x=x_n} \tag{3.19}$$

The LUT inputs are SOC and temperature, while the outputs are the 2-RC circuit parameters and U_{OCV}. These parameters will be fed into the terminal voltage calculation module to calculate the voltages U_1, U_2 on the circuit, the final voltage is derived from the difference between the open circuit voltage and U_1, U_2, I, R_0.

4. SIMULATION RESULT

In this section, the performance of both methods is verified and compared at JE05 conditions.

4.1 Identified Parameters

After the 1D battery model is established, then use the model to conduct the HPPC (Hybrid Pulse Power Characteristic) test to investigate the dynamic characteristics of the battery. The optimization target is the experimental data obtained during the 119A constant current 1C discharge process; the optimized parameters are shown in Table 1 below, and the optimized results are shown in Figure 7.

Table 1 Optimized Parameters Result

Parameter	Unit	Optimized Value
Cathode Thickness	μm	90
Anode Thickness	μm	85
Cathode Porosity	-	0.32
Anode Porosity	-	0.3
Cathode First Charge Capacity	mAh / g	170
Cathode First Discharge Capacity	mAh / g	160
Anode First Charge Capacity	mAh / g	372
Anode First Discharge Capacity	mAh / g	350
Operational Capacity	Ah	119.72
Number of Parallel Cells	-	6

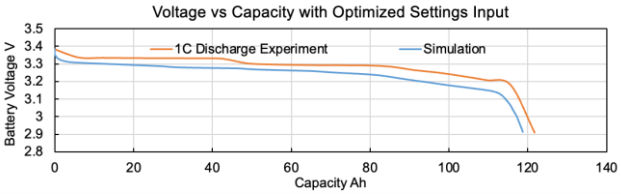

Fig. 7 Terminal Voltage Under 1C Discharge after Optimized

There are approximately 20 parameters that could affect the accuracy significantly withing P2D model. Conducting iterative optimization and defining the optimal range for each parameter can be time-consuming. Therefore, a sensitivity analysis is essential to identify the most influential parameters and enhance the efficiency of the optimization process, can be seen in Figure 8.

The terminal voltage of the optimized P2D electrochemical battery model was compared against chassis dyno test data. The simulation results demonstrated a high degree of accuracy, with a Mean Absolute Percentage Error (MAPE) of 1.21% and a Root Mean Square Error (RMSE) of 0.051 V over the state-of-charge

(SOC) range from 100% to 5% under the predefined current condition. This indicates strong agreement between the simulated and experimental results, with the low MAPE reflecting the improved predictive capability of the model.

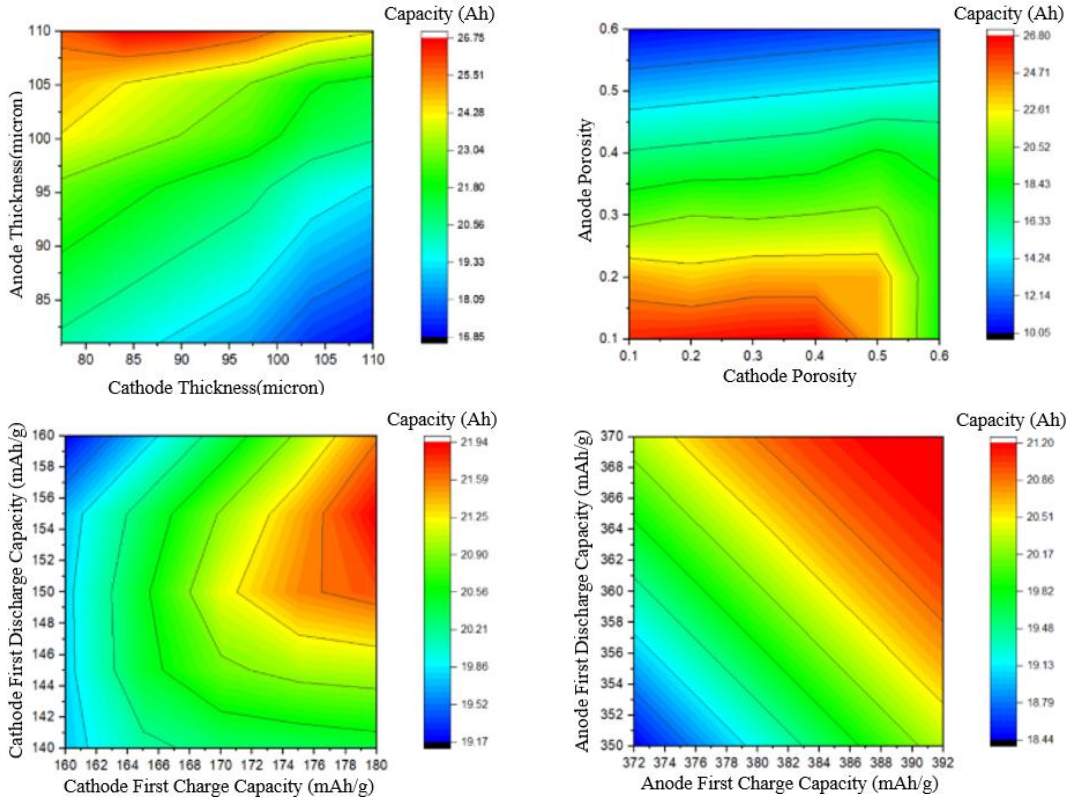

Fig. 8 Sensitivity Analysis of Different Battery Parameters: (a) Sensitivity Analysis of Thickness (b) Sensitivity Analysis of Porosity (c) Cathode First Charge/Discharge Capacity (d) Anode First Charge/Discharge Capacity

After the virtual test and parameters generated, the results were processed to a 2D LUT to extract the equivalent circuit parameters under varying conditions. The LUT takes SOC and temperature as inputs, with SOC ranging from 10% to 90% with a 10% interval and temperature ranging from 298 K to 323 K with a 10 K interval, with the RC circuit parameters and the open-circuit voltage as outputs. These extracted parameters are then fed into the terminal voltage calculation module, where the voltage drops U_1 and U_2 across the RC elements are computed using Equation (3.11). The final terminal voltage is determined as the difference between the open-circuit voltage and the sum of U_1, U_2, I and R_0.

The battery parameters must be characterized separately for charging and discharging conditions since electric vehicle batteries experience alternating current directions in real-world operation. Figures 9 and 10 compare the optimized parameters with the original look-up table under charging and discharging conditions.

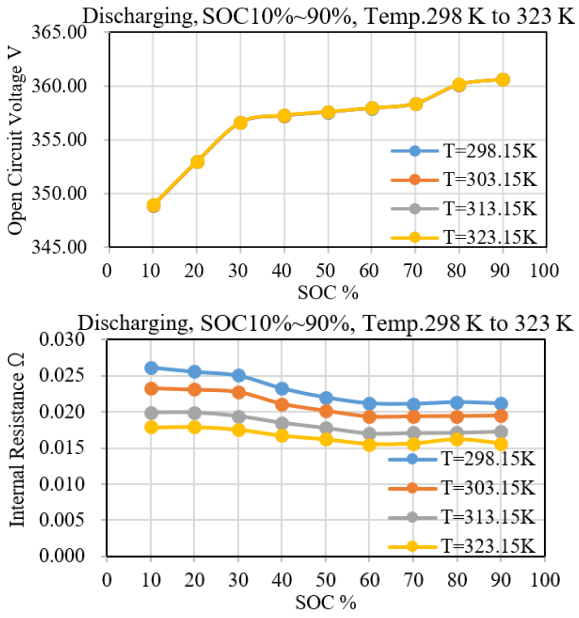

Fig. 9 OCV and IR Comparison during Discharging

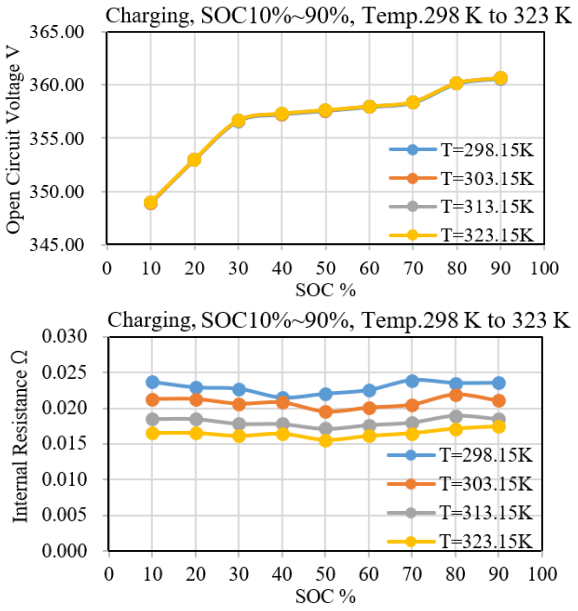

Fig. 10 OCV and IR Comparison during Charging

The double R–C model was selected due to its optimal balance between computational efficiency and accuracy. The identified parameters include two polarization resistances (R1 and R2), as shown in Figures 11 and 12, representing ohmic polarization caused by internal resistances at the interfaces of electrolytes, electrodes, separators, conductive foils, and casings. Additionally, two polarization capacitances (C1 and C2), shown in Figures 13 and 14, represent electrochemical polarization, reflecting the kinetics of lithium-ion reactions at the electrode interface.

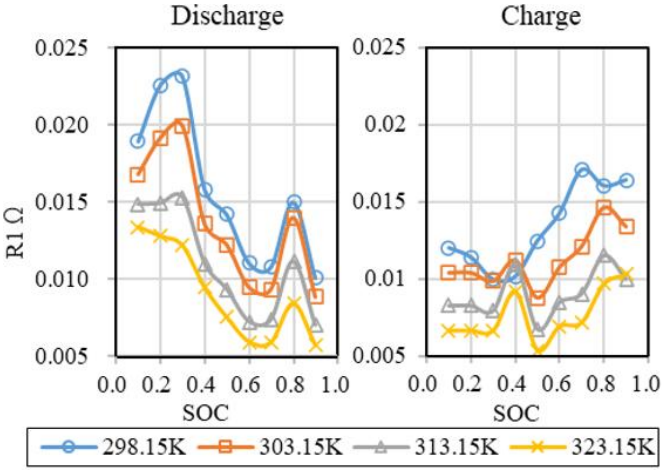

Fig. 11 R1 under different Temperatures, SOCs and Currents

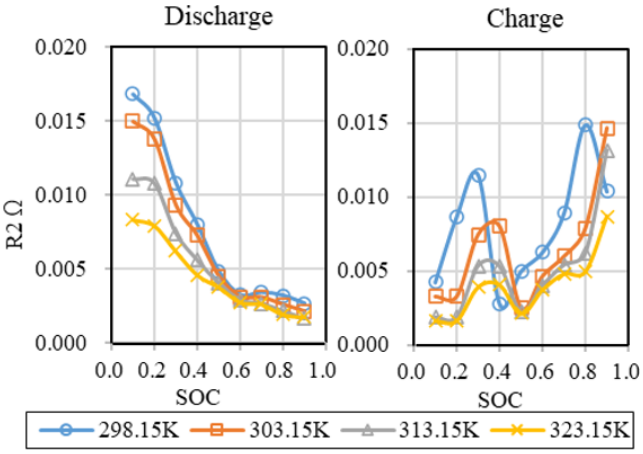

Fig. 12 R2 under different Temperatures, SOCs and Currents

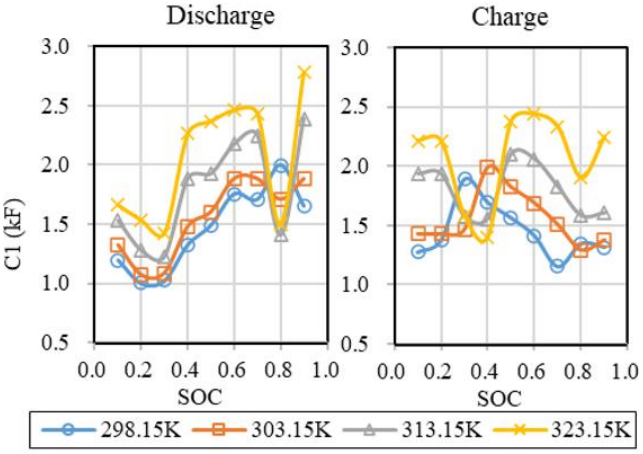

Fig. 13 C1 under different Temperatures, SOCs and Currents

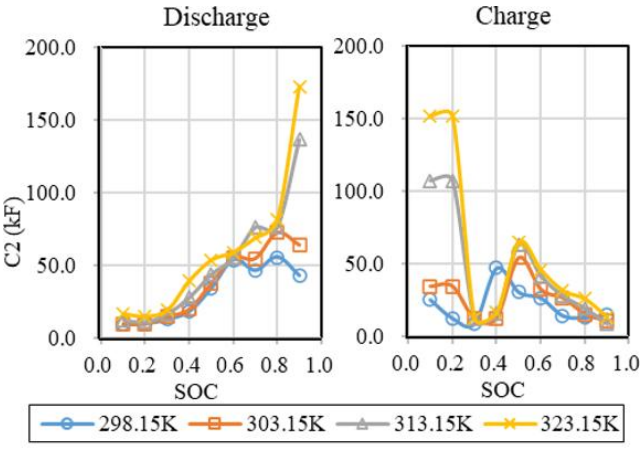

Fig. 14 C2 under different Temperatures, SOCs and Currents

4.2 Validation by Drive-cycles

Figure 15 shows the JE05 drive cycle, conducted at a room temperature of 25 °C and the SOC at 80%. Figure 16 shows the corresponding current coming from three different specifications (S/M/L size) of vehicle of different loads; more details shown in Table 2. Figure 17 shows the simulated voltages plotted against experimental voltages, demonstrating a high correlation between the simulation and experimental data sets. According to the JH25 standard, model validation primarily focuses on the accuracy during the first 121 seconds of the JE05 cycle. The proposed electrochemical-thermal model shows a significant improvement in prediction accuracy within this evaluation period. Table 3 below provides an overall result of the comparison, although a voltage

deviation is observed at the high-speed peak around 1500 seconds, this difference can be attributed to increased thermal dynamics and parameter sensitivity at high load conditions. Nevertheless, the overall error remains within an acceptable range, as confirmed by the low MAPE value. Table 3 below provides an overall result of the comparison.

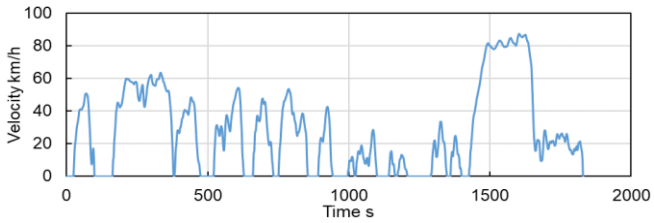

Fig. 15 JE05 Driving Profile

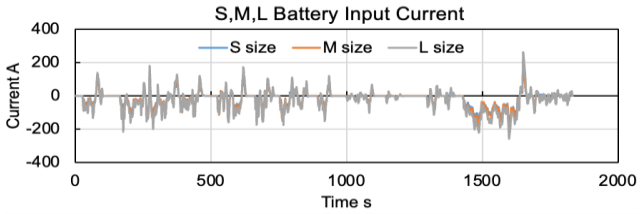

Fig. 16 Corresponding Current of three different specifications

Table 2 Specifications for JH-25 tests

Parameter	Specification/ Value
Ambient Temperature	25degC
Initial SOC	80%
Number of cells	108 in series (348 V nom.)
Energy	41.3 kWh (1 pack)
Cooling type	Liquid, bottom cooling
Weight (est.)	359 kg
Num. of variants	1, with 3 configs: S size: x1 pack, M size: x2 packs, L size: x3 packs

As presented in Table 3, the coefficient of determination (R^2) shows varying degrees of improvement across all three battery pack sizes. Among them, the S-size battery pack exhibits the highest temperature rise, primarily due to its smaller size, which results in a higher current density during charge and discharge cycles, thereby leading to greater heat accumulation. Notably, after 1500 seconds, as shown in Figure 18, the increase in vehicle speed induces sharp current fluctuations, further intensifying the battery's thermal response.

As the vehicle transitions into the high-speed phase, the power demand increases accordingly, leading to a rise in battery heat generation. However, the L-size and M-size battery packs exhibit comparatively lower temperatures.

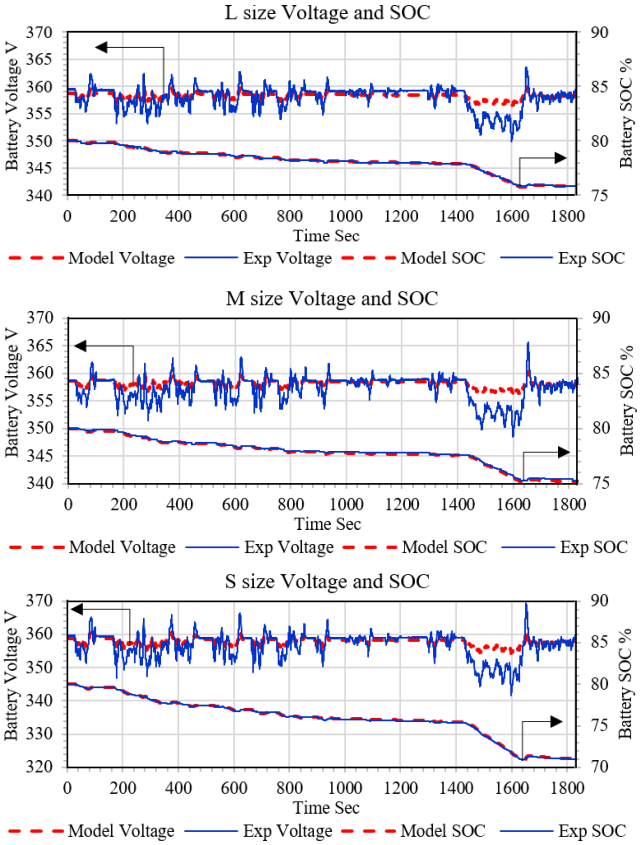

Fig. 17 Battery Voltage Results Comparison

Table 3 Overall Result of the Comparison

Battery pack Size	R^2 W/O thermal	R^2 with thermal	Accuracy improved	MAPE With thermal
L	91.00%	94.80%	3.80%	0.32%
M	88.70%	98.71%	10.01%	0.36%
S	77.00%	99.02%	22.02%	0.585%

*R^2 W/O thermal is using the look-up method according to the interim IR table (W/O thermal)

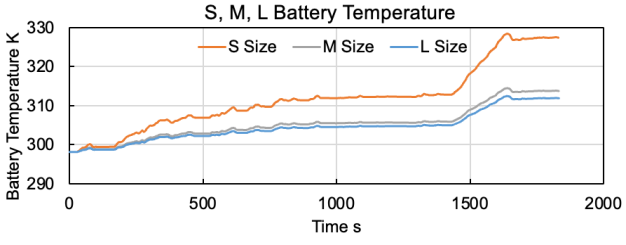

Fig. 18 Temperature Change of the Battery

This can be attributed to their larger capacity, which allows the current to be distributed more evenly, thereby reducing overall heat accumulation. Moreover, the input current remains relatively stable with minimal fluctuations, indicating that the batteries experience lower thermal stress under these conditions.

5. CONCLUSION

This study proposes an advanced electrochemical battery model, that is temperature-dependent and was compared to the conventional internal resistance (IR) look-up table method. The results from the simulation proved that electrochemical modeling predicts a much higher precision value, particularly under varying temperature conditions. Because of its enhanced reliability, the developed model presents a valuable tool for optimizing electric truck performance and energy management systems. The future work will focus on its implementation into an overall vehicle model for HILS testing.

Firstly, the research investigated the accuracy of the original JH25 battery model in simulation. The simulated voltage reached over 88% accuracy at L-size and M-size battery packs for the first 121 seconds, matching one of the target accuracy thresholds. However, for the S-size battery pack, the experimental data showed a lower accuracy within the same time frame. This is because the method's drawback that did not consider the effect of temperature, a key point to be considered in battery performance. Furthermore, the limited parameterization SOC range available in the dataset precluded a thorough evaluation of the dynamic characteristics of the battery.

In order to avoid those drawbacks, a virtual Hybrid Pulse Power Characterization (HPPC) test was implemented through GT-Autolion. An optimized 1D-P2D electrochemical battery model was built with a generation of the appropriate 2-RC equivalent circuit parameters. This battery model incorporated with the thermal sub-model considers heat convection between the battery surface and the coolant circuit. In this case, the battery's internal heat generation and convective heat transfer were used to compute battery temperature, which was then utilized to update the 2-RC model parameters and calculate the output terminal voltage. This enhanced model achieved a voltage prediction accuracy exceeding 98%, significantly outperforming the original JH25 model.

In future research, improved experimental testing and real-world validations are needed. To enhance the comprehensive understanding of battery performance, future work can include battery pulse tests over a wider range of temperature and SOC conditions. Also, further on-road testing under different ambient temperatures is necessary to validate battery models at realistic operating conditions.

ACKNOWLEDGMENT

This work results from a joint research supported technically and financially by Mitsubishi Fuso Truck and Bus Corporation.

REFERENCES

(1) "Global Electric Truck Market By Propulsion, By Vehicle Type, By Range, By Region and Companies - Industry Segment Outlook, Market Assessment, Competition Scenario, Trends and Forecast 2023-2032." Market.US. https://market.us/report/all-electric-trucks-market/ (accessed July 04, 2024).

(2) "Notification Specifying Details of Safety Standards for Road Transport Vehicles." MLIT. https://www.mlit.go.jp (accessed May 05, 2024).

(3) Hu, Y., Yurkovich, S., Guezennec, Y., Yurkovich, B. J. Electro-thermal battery model identification for automotive applications. Journal of power sources. 2011, vol. 196, no. 1, p. 449–457.

(4) Smith, Kandler, Kim, Gi-Heon, Darcy, Eric, Pesaran, Ahmad. Thermal/electrical modeling for abuse-tolerant design of lithium ion modules. International journal of energy research. 2010, vol. 34, no. 2, p. 204–215.

(5) BERNARDI, D., PAWLIKOWSKI, E., NEWMAN, J. A General Energy Balance For Battery Systems. Journal of the Electrochemical Society. 1985, vol. 132, no. 1, p. 5–12.

(6) E. Cui, "A Real-time Thermal Management System Model for Battery Electric Trucks," 2024.

(7) Ma, Y., Sok, R., et al., "Development and Validation of a Battery Thermal Management Model for Electric Vehicles under Cold Driving," SAE Technical Paper 2023-01-1610

(8) Xiong. R, "The core algorithm of power battery management system," *Beijing: Machinery Industry Press*, 2022

(9) J. Kuchly, A. et al. "Li-ion battery SOC estimation method using a Neural Network trained with data generated by a P2D model," *IFAC-PapersOnLine*, vol. 54, no. 10, pp. 336-343, 2021.

(10) Sok, R. et al., "A Methodology to Develop and Validate a 75-kWh Battery Pack Model with Its Cooling System under a Real Driving Cycle," SAE Technical Paper 2024-37-0012.

(11) Sok, R. et al., "Global Sensitivity Analysis on Parameter Identifications of Electrochemical Li-Ion Cell Model Using Transient Test Data Scaled from Battery Electric Vehicle Experiments," SSRN: http://dx.doi.org/10.2139/ssrn.5027287, 2024.

(12) J. S. Newman and N. P. Balsara, Electrochemical systems, Fourth edition. in The Electrochemical Society series. Hoboken, NJ, USA: John Wiley & Sons Inc, 2021.